Observation of the reversibility of a covalent pyrrolobenzodiazepine (PBD) DNA adduct by HPLC/MS and CD spectroscopy†

Khondaker M. Rahman,[a] Colin H. James[a] and David E. Thurston*[a,b]

Pyrrolobenzodiazepines (PBDs) are sequence-selective DNA minor-groove binding agents that covalently bond to guanine with a reported preference for Pu-G-Pu sequences (Pu = Purine). Using HPLC/MS and Circular Dichroism (CD) methodologies, we have established for the first time that the aminal bond formed between PBD molecules and DNA is reversible. Furthermore, we have shown that while the rate of aminal bond cleavage does not depend on the sequence preference of a PBD molecule for a particular binding site, the rate of re-formation of the PBD-DNA adduct does. We have also shown that the PBD anthramycin (**2**) appears to be an exception to this rule in that, during cleavage from the DNA, its C-ring aromatizes and it cannot then re-attach due to a loss of electrophilicity at the C11-position. Although the C-ring aromatization of anthramycin has been previously reported to occur in the absence of DNA and after treatment with trifluoroacetic acid (TFA), in this case no pH lowering was required, with the DNA itself appearing to catalyse the process.

Introduction

Pyrrolo[2,1-*c*][1,4]benzodiazepines (PBDs) are sequence-selective DNA minor-groove binding agents (Fig. 1A).[1–5] They have a chiral centre at their C11a(*S*)-position which provides them with an appropriate 3D shape to fit securely within the DNA minor-groove.[3] In addition, they possess an electrophilic N10–C11 moiety (*i.e.*, interconvertible imine, carbinolamine or carbinolamine methyl ether functionalities) that can form a covalent aminal bond between their C11-position and the nucleophilic C2–NH$_2$ group of a guanine base (Fig. 1B).[3] A range of synthetic PBDs of extended length have been developed by linking non-covalent minor-groove binding components to the C8-position of the PBD A ring (*e.g.*, GWL-78,[5] **1**) or by dimerisation of two monomeric PBD units through their C8-positions to afford PBD dimers (*e.g.*, SJG-136).[6] PBD monomers such as anthramycin (**2**) typically span three base pairs of DNA with a reported preference for 5′-Pu-G-Pu-3′ sequences,[7,8] although more recent data have suggested this sequence preference may be less definitive than previously thought.[9] PBDs have been shown to mediate a number of biological effects including the inhibition of endonucleases,[10] RNA polymerase[11,12] and transcription factor binding.[13] For this reason, there is interest in using PBDs as part of a small-molecule

strategy to target specific DNA sequences for potential use in novel anticancer and antibacterial therapies. Anthramycin (**2**) was the first PBD to be isolated and characterized,[14] and its structure confirmed by X-ray crystallography.[15] Since then, numerous other structurally-related sub-families[5] have been isolated from different *Streptomyces* and *Micrococcus* species, providing a diversity of structures based on the core pyrrolobenzodiazepine scaffold but distinguished from anthramycin by the type and position of substituents in the A- and C-rings, and the degree and position of points of unsaturation in the C-ring. Numerous series of synthetic A- and C-ring substituted PBDs have been reported to have significantly greater antitumour and antibacterial properties than the naturally-occurring molecules,[11,16] and a significant amount of SAR data are now available. The study reported here is based on anthramycin and GWL-78[11] (**1**), a C8-linked PBD *bis*-pyrrole conjugate with promising potential as a gene targeting antitumour agent. GWL-78 has been shown to successfully penetrate cells and interact with DNA sequences important for cell cycle progression.[13] In particular, it can displace and/or inhibit binding of the NF–Y transcription factor to CCAAT motifs within the topoisomerase IIα promoter region thus resulting in decreased topo IIα expression. This blocks cell cycle progression and leads to the induction of apoptosis.[13]

It has previously been demonstrated that denaturation of a PBD-DNA adduct either by heat or enzymatic degradation can lead to the loss of up to 70% of bound ligand due to a change in the secondary structure of DNA.[17] Until our present study, it had been assumed, but never demonstrated, that PBD-DNA adducts might be reversible, and that cooling after heating may result in re-formation of the aminal bond. In a related study, Hurley and co-workers showed that after treating anthramycin

[a]Gene Targeting Drug Design Research Group, The School of Pharmacy, University of London, 29/39 Brunswick Square, London, WC1N 1AX, UK. E-mail: david.thurston@pharmacy.ac.uk
[b]Spirogen Ltd, The School of Pharmacy, University of London, WC1N 1AX, UK
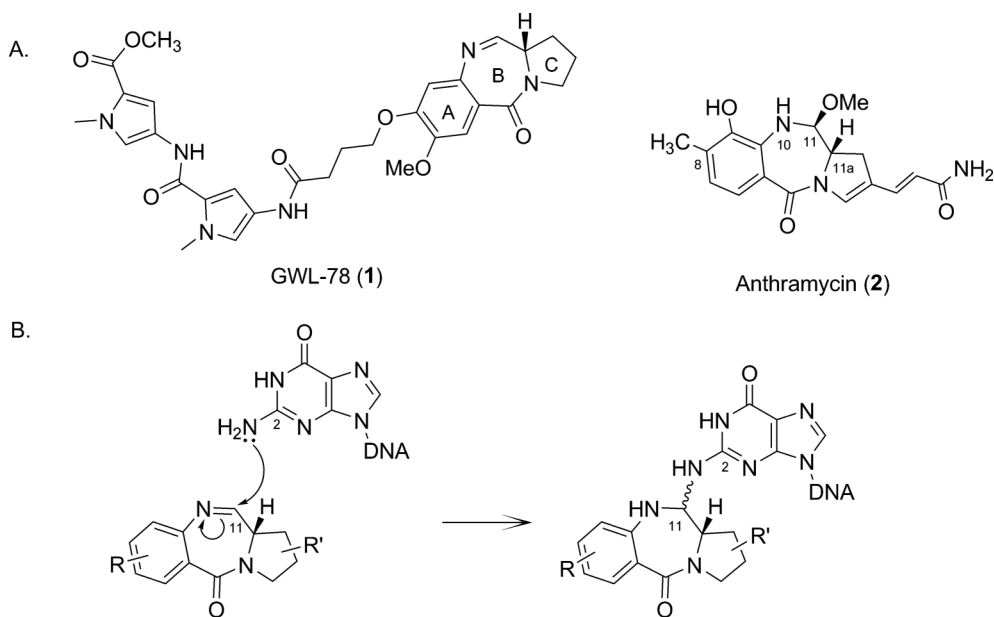
Fig. 1 A, Structures of the C8-*bis*-pyrrole PBD conjugate GWL-78 (1) and the naturally-occurring anthramycin (2). B, Schematic diagram of the mechanism of covalent binding of a PBD through its electrophilic C11-position to the C2–NH$_2$ of a guanine base within the DNA minor groove.
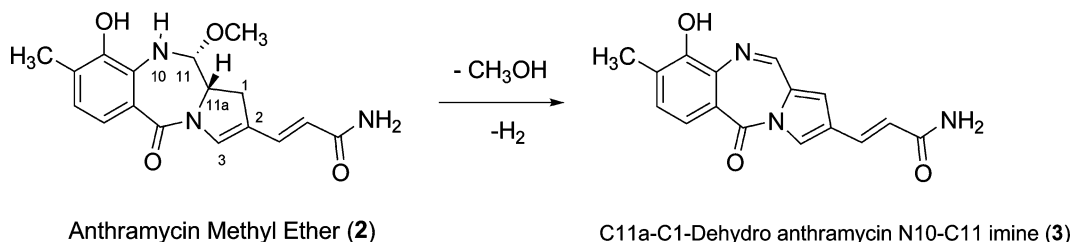
Scheme 1 Formation of the non-electrophilic C11a–C1-dehydro N10–C11-imine analogue (3) of anthramycin (2).

with trifluoroacetic acid, it is converted to the non-electrophilic C11a–C1-dehydro analogue 3 (Scheme 1)[17] that is no longer able to bond covalently to DNA. In the present study we have re-investigated anthramycin (2) in this context, and compared it to GWL-78 (1) which is not prone to C-ring aromatization.

We recently reported the dynamic nature of a hairpin DNA structure when covalently attached to a PBD molecule.[18] These studies demonstrated the ability of a PBD molecule to remain attached to a hairpin DNA fragment despite a loss of minor groove structure during the transition process. This led us to investigate the effect of heat-induced loss of minor groove structure on PBD-DNA adduct stability using HPLC/MS[19,20] and polarised light spectroscopy. Interestingly, in the case of heat-induced detachment of GWL-78 (1) from DNA, we found that although the rate of aminal bond cleavage upon heating does not depend on the DNA sequence around the covalent binding site, the rate of re-formation of the adducts did depend on sequence context. GWL-78 (1), which has an AT-preferring C8-*bis*-pyrrole side chain and a C-ring that is not prone to aromatization, rapidly reformed an adduct with AT-rich oligonucleotides whereas adduct re-formation was slow and incomplete with GC-rich oligonucleotides which are not well-tolerated by the *bis*-pyrrole side-chain. We also observed that N10–C11 imine formation and subsequent aromatization of anthramycin (2) to its non-electrophilic C11a–C1-dehydro analogue followed by ejection from the DNA helix occurred

spontaneously upon heating, whereas this chemical conversion has been previously reported to require treatment with TFA.[21] These results add to chemical knowledge of PBD-DNA adducts, and could be important for the future interpretation of gel-based assays in which PBD/DNA adducts are subjected to a heating step.

Results and Discussion

The HPLC study was carried out using the oligonucleotides shown in Table 1, and an HPLC assay utilizing an X-Terra MS C18 2.5 µM column (4.6 × 50 mm), a gradient of 40% acetonitrile–water and 100 mM TEAB/water as mobile phase, a flow rate of 0.5 ml min^{-1}, UV detection at 254 nm and a 4 : 1 molar ratio of ligand : oligonucleotide. HPLC fractions were collected, combined when appropriate, lyophilised and subjected to MALDI TOF MS to identify constituents.

Annealed *Seq-1* gave a single peak in the HPLC chromatogram at RT 27.1 min which was collected and identified by MALDI-TOF-MS (Fig. 2A). Incubation of *Seq-1* with GWL-78 (1) followed by immediate injection ($\cong$ 5 mins) onto the HPLC column resulted in the appearance of a new peak at RT 28.8 min (Fig. 2B). A time course study showed rapid conversion to this peak with reaction essentially complete (~95%) after 3 h and complete disappearance of the DNA peak (Fig. 2C). No further changes

Table 1 Structures and average masses of the single-stranded (SS) oligonucleotides used in the study, and the average masses of the adducts formed after their covalent interaction with **1** or **2**

Label	SS DNA Sequence	Average Mass of SS DNA	Average Mass of 1:1 **1**/Hairpin DNA Adducts	Average Mass of 1:1 **2**/Hairpin DNA Adducts
Seq-1	5′-TATAAGATTTTCTTATA-3′	5173.45	5764.12	5470.76
Seq-2	5′-GCGCAGATTTTCTGCGC-3′	5175.45	5768.04	5472.76
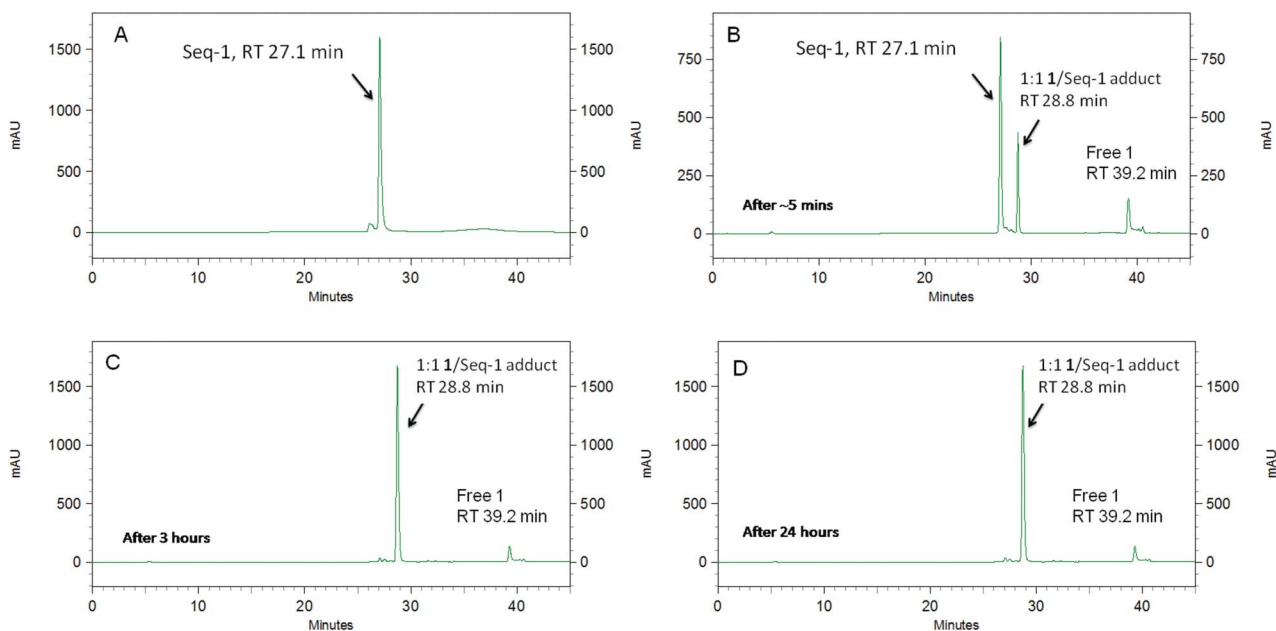
Fig. 2 HPLC chromatograms: **A**, **1**/*Seq-1*, retention time 27.1 min; **B**, *Seq-1* immediately after incubating with **1** (approx. 5 min), gradual appearance of the 1:1 *Seq-1* adduct at 28.8 min; **C and D**, *Seq-1* after incubating with **1** for 3 h and 24 h, respectively. Formation of the **1**/Seq-1 adduct is complete after 3 h.

were observed after 24 h (Fig. 2D). The adduct peak at RT 28.8 min was collected, subjected to MALDI-TOF-MS, and identified as the 1:1 **1**/*Seq-1* adduct.† Similarly, *Seq-1* (Fig. 3A) was incubated with **2**, and immediate HPLC analysis (≅ 5 min) revealed the appearance of a minor peak at RT 26.4 min (Fig. 3B). Unlike the first study with **1**, reaction between **2** and *Seq-1* was slow, with adduct formation only complete after 20 h (Fig. 3C and 3D). Interestingly, the 1:1 **2**/*Seq-1* adduct peak had a shorter retention time than the oligonucleotide alone, contrasting with all other pyrrolobenzodiazepines examined using this HPLC-MS assay.[19,20,22] The identity of the adduct peak at RT 26.4 min was confirmed by MALDI-TOF-MS, ESI.†

To investigate the reversibility of the PBD-DNA adducts, **1** and **2** were incubated separately with *Seq-1* and the solutions left for 24 h to ensure complete covalent reaction. HPLC analysis of the post-24 h incubation samples showed only the presence of the adduct peaks which were identified by MALDI-TOF MS (*e.g.*, Fig. 4A for **1**/*Seq-1*). Initially, the **1**/*Seq-1* incubation mixture was heated to 90 °C over a period of 10 min using a Grant incubator and then placed on ice. Immediate injection of the incubation mixture onto the HPLC column (≅ 5 min) revealed that >90% of the adduct had reverted back to the DNA peak and free PBD indicating that **1** had detached from the DNA (Fig. 4B). This was consistent with a previous report that attributed the loss of up to 70% of a covalently attached PBD after heating to a loss of

DNA minor groove structure.[17] The **1**/*Seq-1* incubation mixture was then left on ice for 10 min before re-injecting onto the HPLC column. In this case (Fig. 4C), the adduct peak (RT 28.8 min) re-appeared (>80%) with a diminished DNA peak at RT 27.1 min. This re-attachment process was complete after a 15 min cooling period (Fig. 4D). These results demonstrated that the PBD-DNA aminal bond cleaved during the heating procedure, but reformed within 10 min after cooling. The speed of this bond re-formation was surprising, as PBDs can take up to 24 h to react with duplex DNA according to the literature, and the reaction between **1** and *Seq-1* initially took 3 h to complete at the beginning of the study. This suggested that, although the PBD-DNA aminal bond cleaved during the heating procedure, the PBD must have remained in close association with the hairpin DNA, perhaps through non-covalent interactions. In the case of **1**, such non-covalent interactions might be facilitated by the C8-*bis*-pyrrole units which are known to have a high affinity for DNA, and particularly for AT rich regions. In this case, once heat is withdrawn and the incubation mixture placed on ice, the reactive C11-position of the PBD may be close enough to the guanine C2–NH$_2$ group to allow adduct re-formation almost immediately.

Next, interaction between **2** and *Seq-1* was studied using the same experimental approach. A post 24 h **2**/*Seq-1* incubation mixture (Fig. 5A and 5B) was heated to 90 °C over a period of 10 min and immediately placed on ice and then analysed by
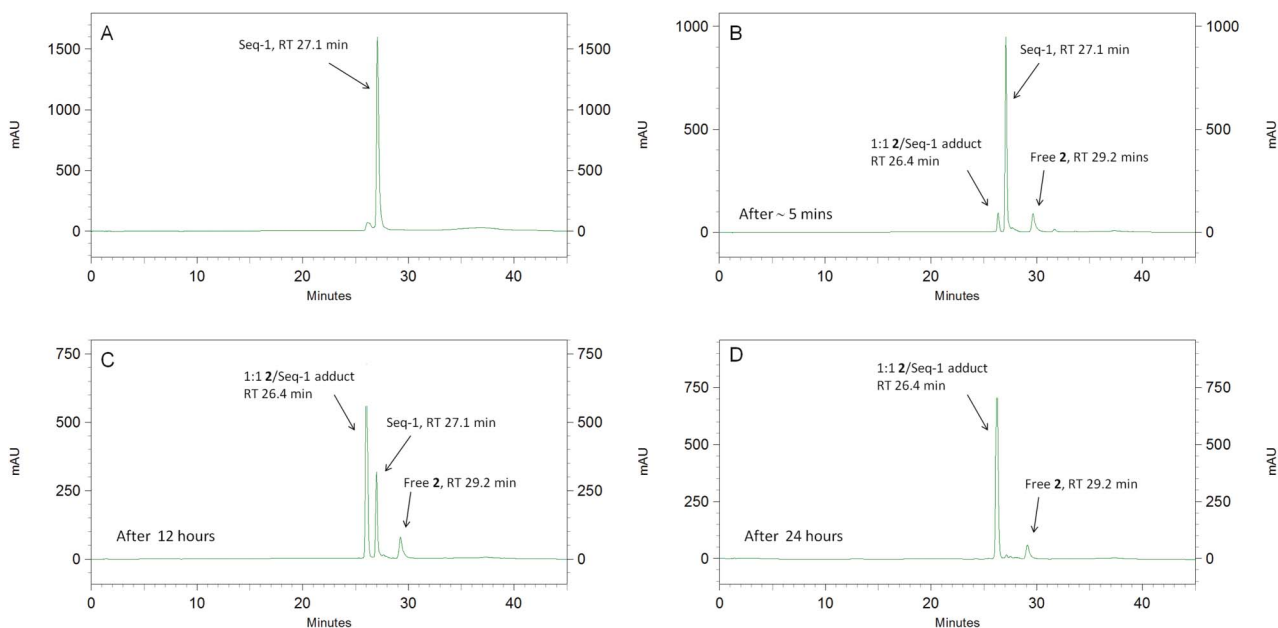
Fig. 3 HPLC chromatograms: **A**, *Seq-1*, retention time 27.1 min; **B**, *Seq-1* immediately after incubating with **2** (approx. 5 min), gradual appearance of the 1:1 **2**/*Seq-1* adduct at 26.4 min; excess free **2** at 29.2 min; **C and D**, *Seq-1* after incubating with **2** for 12 h and 24 h, respectively. Formation of the **2**/*Seq-1* adduct is complete after 24 h.
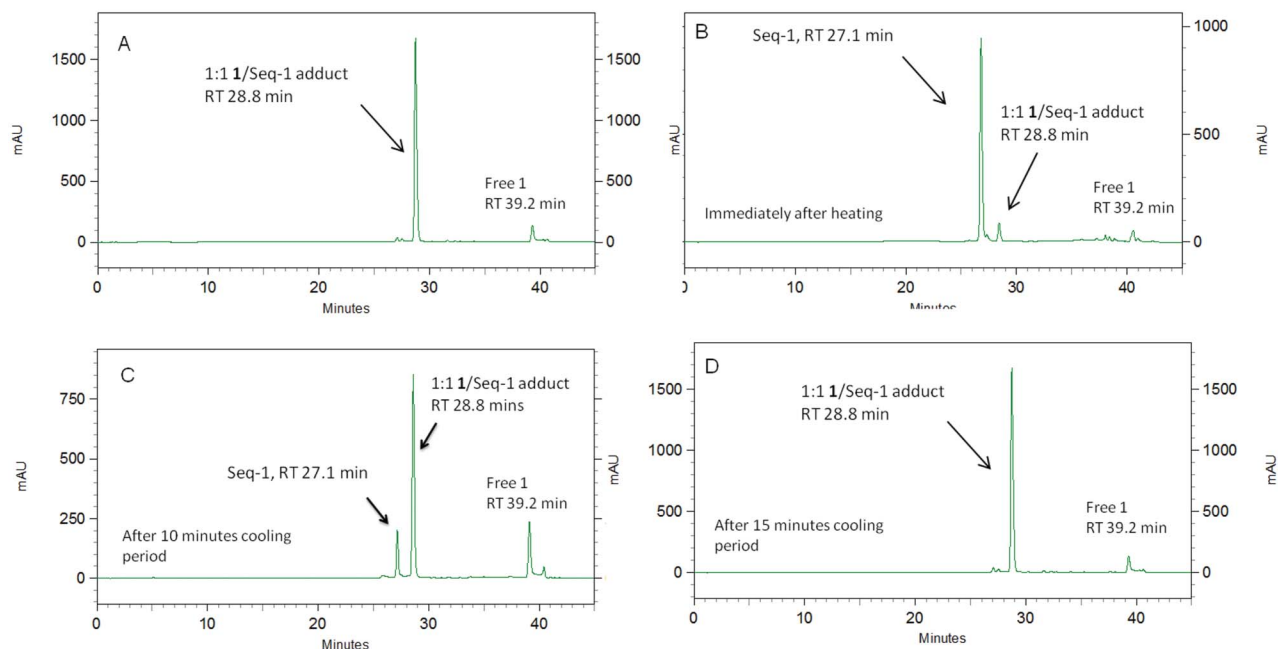
Fig. 4 HPLC chromatograms: **A**, *Seq-1* after incubating with **1** for 24 h showing the 1:1 **1**/*Seq-1* adduct at 28.8 min; excess free **1** at 39.2 min; **B**, 1:1 **1**/*Seq-1* adduct immediately after heating to 90 °C. **C and D**, 1:1 **1**/*Seq-1* adduct after post-heating 10 and 15 min cooling periods, respectively. Adduct re-formation was complete after 15 min.

HPLC. The chromatogram (Fig. 5C) showed only a small amount of adduct at RT 26.4 min ($\cong$ 5%) and a DNA peak at RT 27.0 min ($\cong$ 95%) indicating that **2** had detached from the DNA. Interestingly, the peak corresponding to **2** that had previously appeared at RT 29.2 min before the heating procedure (Fig. 5A and 5B) now appeared at a slightly increased retention time of 29.9 min.

This peak was collected, and EI-MS (see ESI†) provided a mass of 295 Da, 34 units lower than anthramycin and consistent with the C11a–C1-dehydro, N10–C11 imine form of anthramycin (**3**, Scheme 1), indicating that a chemical conversion had occurred during the heating process. Hurley and co-workers had previously reported this chemical conversion when anthramycin alone was

This journal is © The Royal Society of Chemistry 2011

Org. Biomol. Chem., 2011, **9**, 1632–1641 | 1635
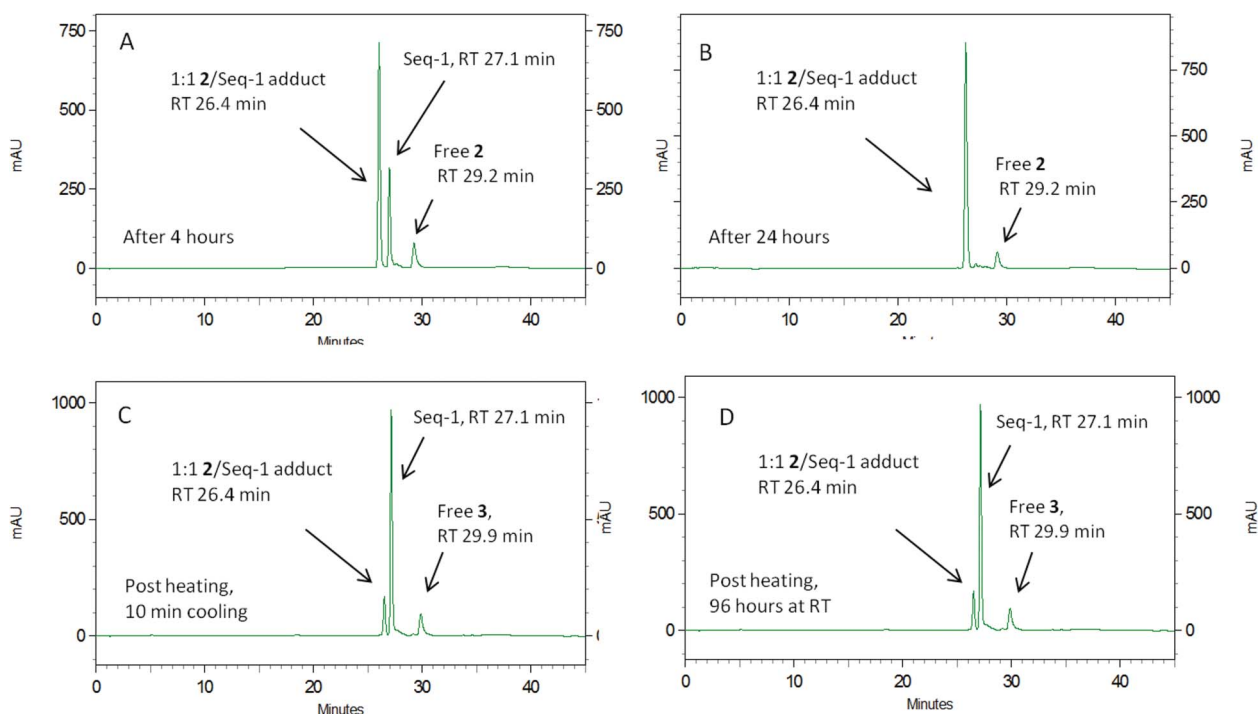
Fig. 5 HPLC chromatograms: **A and B**, *Seq-1* after incubating with **2** for 4 h and 24 h, respectively, showing the 1 : 1 **2**/*Seq-1* adduct at RT 26.4 min and excess free anthramycin at RT 29.2 min; **C and D**, 1 : 1 **2**/*Seq-1* adduct after 10 min post-heating cooling and 96 h post-heating storage at room temperature, respectively, showing that most of the adduct had reverted to *Seq-1* DNA and a new peak at RT 29.9 min identified by MS as the C1–C11a-dehydro N10–C11-imine anthramycin derivative (**3**). The adduct did not re-form even afer 96 h (as shown in **D**).

treated with TFA,[21] but in this case the same reaction was observed while **2** was covalently attached to DNA and heated in 100 mM Na acetate buffer (pH 6.93). As a control, anthramycin was heated to 90 °C in the same buffer, and left at RT for 6 h. However, no change to the anthramycin occurred, indicating that the presence of DNA was required which appeared to be acting as type of catalyst. As anticipated, the adduct peak did not re-appear when the incubation mixture was left on ice for 10 min (Fig. 5C) or after 96 h incubation at RT (Fig. 5D), thus confirming the lack of reactivity of the C11a–C1 dehydro analogue (**3**). Furthermore, MALDI-TOF-MS analysis of the RT 27.1 min peak collected from the HPLC analyses of both pre- and post-heating incubation mixtures showed no change in mass for *Seq-1*. Finally, leaving the **2**/*Seq-1* adduct to stand at room temperature for 48 h resulted in a mixture of anthramycin (**2**) and C11a–C1 dehydro anthramycin (**3**) (approximately 1 : 1) demonstrating that the reaction can occur at room temperature after a longer incubation time.

We next studied the interaction of **1** and **2** with the GC-rich *Seq-2* to investigate sequence preference. Annealed *Seq-2* gave a single peak at RT 24.4 min which was collected and identified by MALDI-TOF-MS (ESI†). Incubation of **1** with *Seq-2* provided a new peak at RT 28.7 min, although reaction was very slow with only 10% conversion to adduct at 0 h (~5 min) and approximately 70% after 24 h. The new peak at RT 28.7 min was collected and identified by MALDI-TOF-MS as the 1 : 1 **1**/*Seq-2* adduct, ESI.† The **1**/*Seq-2* 24 h incubation mixture was heated to 90 °C over a period of 10 min, then placed on ice and a sample immediately analysed by HPLC. This showed that almost all the 1 : 1 **1**/*Seq-2* adduct had reverted back to DNA and ligand. However, when this heated mixture was left to stand on ice for 10 min, a small

(5%) increase in the adduct peak was observed. This contrasted significantly with the **1**/*Seq-1* heating-cooling experiment in which approximately 90% of the 1 : 1 **1**/*Seq-1* adduct had re-formed within 15 min. A post heating/cooling time-course experiment showed that approximately 26 h was required to regain the same amount of 1 : 1 **1**/*Seq-2* adduct present at the start of the experiment, ESI.† This lower rate of adduct re-formation compared to the **1**/*Seq-1* experiment was assumed to be due to the relative lack of affinity of the C8-*bis*-pyrrole unit of GWL-78 (**1**) for GC base pairs, resulting in the molecule not staying closely associated with the DNA after detachment.

A similar experiment with **2** and *Seq-2* proceeded as expected with no significant difference from the results obtained for **2**/*Seq-1*, other than slower adduct formation. Reaction was incomplete after 24 h and, once anthramycin had detached from the DNA as the C11a–C1 dehydro form (**3**) after heating, no re-attachment was possible consistent with the **2**/*Seq-1* experiment. This further confirmed the chemical conversion of **1** to the non-electrophilic C11a–C1 dehydro form (**3**) in the presence of buffer and nucleic acid.

Molecular modelling studies were carried out to help understand the various rates of adduct formation for the different ligands and oligonucleotides. Energy minimized structures for both **1**/*Seq-1* and **2**/*Seq-1* (Fig. 6) showed that both molecules become embedded within the minor groove due to their unique 3-dimensional shapes based on the stereochemistry at their C11a positions. In the case of GWL-78 (**1**), the model shows that the ligand spans five base-pairs in the stem of the DNA hairpin, with the C8-*bis*-pyrrole side-chain lining-up with the A/T base pairs adjacent to the covalent binding site (Fig. 6A). On the other hand,
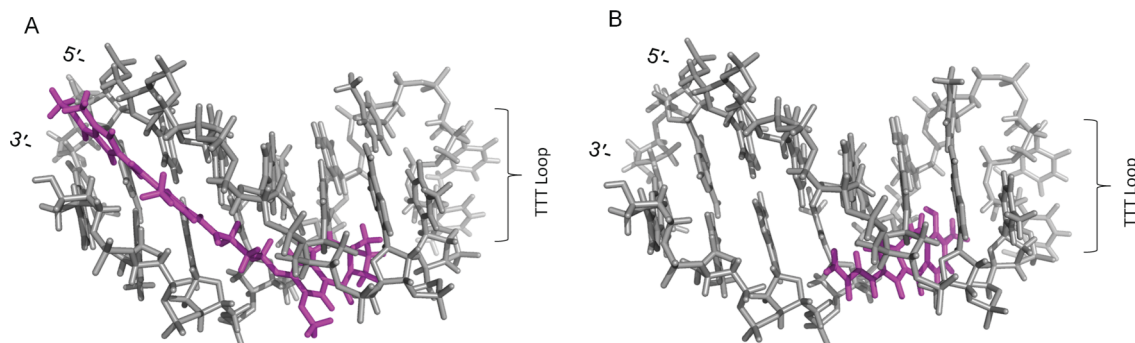
Fig. 6A and 6B: Energy minimized molecular models of GWL-78 (**1**) and anthramycin (**2**), respectively, covalently bound to *Seq-1*. (**A**) GWL-78 (**1**) extends over five base pairs with the C8-*bis*-pyrrole side chain oriented to the 5′-end, aligning and interacting with the A/T base pairs to provide a high level of stability. The rapid nature of adduct formation between GWL-78 and *Seq-1* can be explained by these additional interactions. (**B**) Anthramycin (**2**) spans only the PBD binding triplet (AGA), but adduct formation with *Seq-1* is still rapid. Note: In the case of *Seq-2*, GWL-78 reacts much more slowly, as interaction of the C8-*bis*-pyrrole side chain with guanine base-pairs is unfavourable, whereas anthramycin maintains reactivity.

anthramycin (**2**) spans only three base pairs and its interaction with other base pairs is limited to the triplet binding site itself (Fig. 6B). Therefore, the model shown in Fig. 6A illustrates the potential additional non-covalent interactions between the C8-*bis*-pyrrole side chain of **1** and the A/T base pairs that are presumably the main driving force for the faster reaction of this ligand compared to **2**. The models also explain the slower adduct formation between **1** and GC-rich *Seq-2*, as the *bis*-pyrrole C8-side chain does not interact favourably with G/C base pairs.

Next, polarized light spectroscopy was used to validate the HPLC/MS data. Circular Dichroism (CD) and UV melting data for the DNA adducts of **1** and **2** were collected over a wide temperature range using an Applied Photophysics Chirascan spectrometer. All spectra were acquired at room temperature and a buffer baseline correction applied. For temperature stability, the CD spectrum was first recorded at room temperature (20 °C), then at the highest temperature (90 °C), and finally after re-cooling to 20 °C. Melting profiles were recorded during both the heating and cooling phases. Both **1** and **2** are chiral molecules due to the C11a(*S*)-stereochemistry, and so have their own characteristic CD signals, ESI.† Also, the CD spectrum of *Seq-1* alone confirmed the presence of a double-helical DNA structure. Incubation of **1** with *Seq-1* at RT for 3 h gave a significant enhancement of the CD signal at 260 nm and a drug-induced enhancement of the signal at 320 nm confirming adduct formation. Titration of *Seq-1* with 1–4 equivalents of **1** showed that the effect was more pronounced at the same 4 : 1 ratio (drug:DNA) as used in the HPLC study (Fig. 7A). A similar CD study with **2** and *Seq-1* also showed a significant concentration-dependent enhancement of CD signals, with a drug-induced CD signal at 360 nm the most prominent (Fig. 7B).

Next, the CD spectrum of the **1**/*Seq-1* incubation mixture (4 : 1) was recorded at 20 °C, and then monitored while heating at a rate of 3 °C min⁻¹ to 90 °C. The incubation mixture was then cooled to 20 °C at the same rate and the CD spectrum re-measured. A comparison of CD spectra at 20 °C, 90 °C and after cooling to 20 °C is shown in Fig. 7C. An induced enhancement of the 320 nm CD signal due to **1** was apparent at 20 °C, but this induced signal was absent in the spectrum recorded at 90 °C, confirming detachment of the PBD from the DNA helix at the higher temperature. However, this signal reappeared in

the CD spectrum after cooling the incubation mixture to 20 °C, indicating re-formation of the **1**/*Seq-1* adduct. These results were consistent with those from the HPLC/MS assay in which adduct re-formation was observed after a 10 min cooling period. As the cooling procedure from 90 °C to 20 °C in the CD experiments occurred over approximately 23 min, it also confirmed the rapid nature of adduct re-formation and supported the hypothesis that **1** most likely remained in close association with the DNA despite cleavage of the covalent bond.

Similar CD experiments were performed with a mixture of **2** and *Seq-1* which was incubated initially for 24 h. The spectrum recorded at 20 °C post-incubation showed the presence of a drug-induced CD peak at 360 nm. However, this was lost after heating the mixture to 90 °C at a rate of 3 °C min⁻¹, indicating that **2** had become detached from the DNA. As anticipated, the CD signal remained absent after cooling to 20 °C (Fig. 7D) indicating that **2** could not re-attach. Re-measurement after 3 h still failed to show the drug-induced CD signal, consistent with the results of the HPLC-MS experiments. Similar CD studies on the 1 : 1 **1**/*Seq-2* and 1 : 1 **2**/*Seq-2* adducts, ESI,† also provided results consistent with the equivalent HPLC/MS experiments. In the case of **1**/*Seq-2*, the drug-induced negative CD signal initially observed at 305 nm disappeared upon heating to 90 °C and then re-appeared after cooling, confirming the reversibility of the adduct. On the other hand, for **2**/*Seq-2*, the drug-induced positive CD signal was initially observed at 360 nm but disappeared after heating to 90 °C. As anticipated, the signal did not re-appear over the course of the experiment, indicating the permanent detachment of anthramycin (**2**) and its conversion to the C-ring aromatized C11a–C1 dehydro analogue (**3**), ESI.†

Comparative thermal denaturation (melting) studies were carried out on all four adducts, and the results are shown in Table 2. The T_m values of the adducts were consistently higher than those of the hairpin DNAs alone, thus confirming that DNA stabilization had occurred upon covalent binding of **1** or **2**. The **1**/*Seq-1* and **2**/*Seq-1* adducts were significantly stabilized to a similar degree (*i.e.*, 42 °C *vs.* 38 °C, respectively), most likely due to the inherently higher affinity of GWL-78 (**1**) for AT-rich sequences due to the attraction of the pyrrole units for AT base pairs, and the much lower sequence-selectivity of anthramycin (**2**)
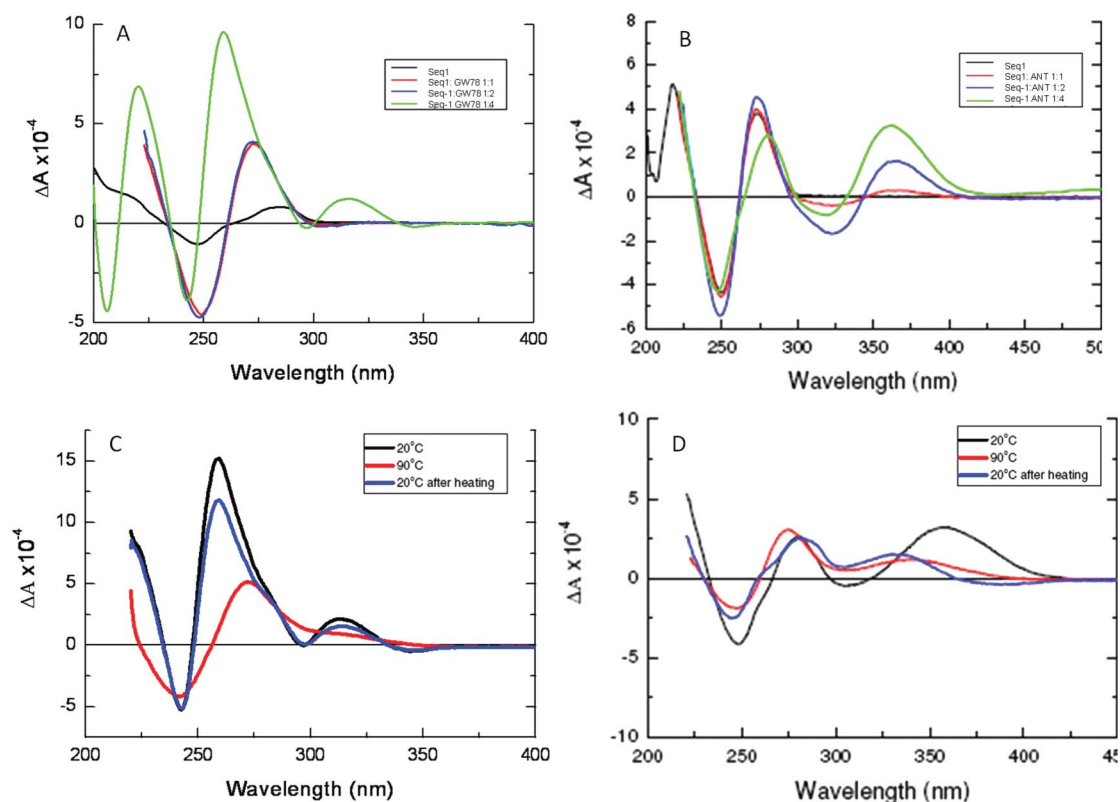
Fig. 7 **A**, CD spectrum of the **1**/*Seq-1* adducts at different DNA/ligand ratios (1 : 1, 1 : 2 and 1 : 4); **B**, CD spectrum of the **2**/*Seq-1* adducts at different DNA/ligand ratios (1 : 1, 1 : 2 and 1 : 4); **C**, CD spectrum of the **1**/*Seq-1* adduct at 20 °C (black), after heating to 90 °C (red), and then after cooling to 20 °C (blue); **D**, CD spectrum of the **2**/*Seq-1* adduct at 20 °C (black), after heating to 90 °C (red), and then after cooling to 20 °C (blue). Note that the ligand-induced CD signal for **1** at 305 nm re-appeared after cooling but the drug-induced CD signal for **2** at 360 nm did not re-appear post-heating, thus confirming permanent detachment of **2** from the DNA.

Table 2 Melting temperatures of the hairpin sequences *Seq-1* and *Seq-2* and their covalent adducts with GWL-78 (**1**) and anthramycin (**2**)

Construct	T_m of DNA hairpin alone (°C).	T_m of DNA hairpin adducts (°C).	ΔT_m (°C)
Seq-1	38	—	—
Seq-2	44	—	—
1/Seq-1	—	80	42
1/Seq-2	—	56	12
2/Seq-1	—	76	38
2/Seq-2	—	75	31

due to its smaller size. Conversely, as anticipated, the **2**/*Seq-2* adduct was stabilised to a significantly greater degree than the **1**/*Seq-2* adduct (31 °C *vs.* 12 °C) due to the poor tolerance of the C8-*bis*-pyrrole unit of **1** for the GC base pairs within *Seq-2*. Results for the temperature/time-course experiments for the **1**/*Seq-1* and **2**/*Seq-1* adducts are shown in Fig. 8, along with the associated cooling data. The non-coincidence of the heating and cooling curves for the adducts is a significant feature, and reflects the detachment of the ligands from DNA at higher temperatures and an inability to re-attach covalently within the time-frame of the experiment. However, it is evident from Fig. 8A that for **1**, the curve has a tendency to return to the original position as the adduct is gradually re-formed, whereas in the case of **2** (Fig. 8B),

the curves remain relatively linear reflecting the inability of the aromatized anthramycin to re-attach.

Conclusion

Using HPLC/MS methodology and polarized light spectroscopy we have demonstrated for the first time that a PBD-DNA adduct formed from a C-ring saturated PBD can dissociate when heated and then re-form upon cooling. Furthermore, we have established that while the rate of initial dissociation of the PBD-DNA adduct is independent of DNA sequence, the rate of adduct re-formation is sequence dependent. Finally, we have demonstrated that anthramycin (**2**), which has C2–C3 unsaturation and is prone to C-ring aromatisation, cleaves from DNA upon heating as the C11-non-electrophilic C-ring-aromatized species (**3**) which cannot react with DNA again. Although this chemical transformation has been previously observed by Hurley and co-workers upon treatment of anthramycin with TFA,[21] in this case the DNA itself appeared to be catalysing the reaction, although the details of the mechanism are not known. Together, these findings add to knowledge of PBD chemistry and DNA adduct formation, and could be important for the correct interpretation of the results of biochemical assays such as DNA footprinting in which adducts are subjected to a heating step.
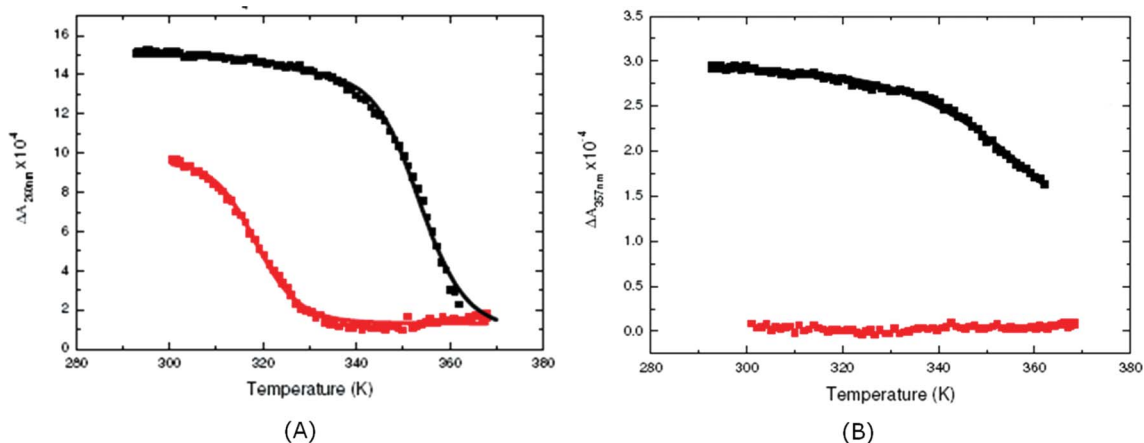
Fig. 8 A, Temperature profile of the **1**/*Seq-1* adduct; heating phase (black) and cooling phase (red); B, Temperature profile of the **2**/*Seq-1* adduct; heating phase (black) and cooling phase (red). Note: Ligand/DNA ratio was 4 : 1 in both cases.

Experimental

HPLC/MS assay

Oligonucleotides. The single-stranded oligonucleotides were purchased from Eurogentec (Southampton, UK) and ATDBio (Southampton, UK) in lyophilised form.

Working Solutions of Hairpin Oligonucleotides. Each oligonucleotide was dissolved in 1 M ammonium acetate (Sigma-Aldrich, UK) to form a stock solution of 1 mM. To ensure hairpin formation, the solutions were heated to 90 °C for 10 min in a heating/cooling block (Grant Bio, UK). The solutions were then allowed to cool slowly to room temperature followed by storage at −20 °C overnight to ensure completion of the annealing process. Working solutions of hairpin oligonucleotides of 50 μM were prepared by diluting the stored stock solutions with 100 mM ammonium acetate. The working solutions were stored at −20 °C and discarded after 4 weeks.

GWL-78 (1) Working Solution. GWL-78 (**1**) was provided by Spirogen Ltd (Batch No. SG2274.005), and was dissolved in methanol–water (2 : 1 v/v) to form a stock solution of 10 mM which was stored at −20 °C for no longer than four months. Working solutions of 200 μM were prepared by diluting the 10 mM stock solution with 100 mM ammonium acetate solution. These were stored at −20 °C for no longer than one week, and thawed to room temperature for use when required.

Anthramycin (2) Working Solution. Anthramycin (**2**) was purchased from Sigma-Aldrich (UK) in powdered form, and its identity confirmed by LC-MS and NMR analysis. It was dissolved in methanol–water (2 : 1 v/v) to form a stock solution of 10 mM which was stored at −20 °C for no longer than four months. Working solutions of 200 μM were prepared by diluting the 10 mM stock solution with 100 mM ammonium acetate solution. These working solutions were stored at −20 °C for no longer than one week, and thawed to room temperature for use when required.

Preparation of Ligand/DNA Complexes. Ligand/DNA complexes were prepared by adding a PBD working solution to a hairpin oligonucleotide working solution (50 μM) in a 4 : 1 molar ratio at room temperature. This incubation mixture was then agitated for 5–10 s using a vortex mixer.

Ion-pair Reversed-Phase HPLC. HPLC analysis was performed on a Thermo Electron HPLC system equipped with a 4.6 × 50 mm Xterra MS C18 column packed with 2.5 μM particles (Waters Ltd, UK), an UV 1000 detector, an AS3000 autosampler, a SCM1000 vacuum degasser and Chromquest software (Version 4.1). A gradient system of 150 mM triethyl ammonium bicarbonate (TEAB) as buffer A and 40% acetonitrile in water (HPLC grade, Fischer Scientific, UK) as buffer B was used. For buffer A, a 1 M pre-formulated solution of TEAB was purchased from Sigma-Aldrich (UK) and diluted to the required concentration with HPLC grade water (Fischer Scientific, UK). The gradient was ramped from 90% A at 0 min to 50% A at 20 min, 35% A at 30 min and finally to 10% A at 45 min. UV absorbance was monitored at 254 nm, and fractions containing separated components were collected manually, combined when appropriate, lyophilised and then analysed using either EI-MS or MALDI-TOF-MS.

Lyophilisation of HPLC Fractions. Single or combined HPLC fractions were lyophilised using two different methods depending on the final volume. For smaller volumes (less than 0.5 mL), lyophilisations were carried out in a SpeedVac (Thermo Electron) using a temperature-free 4 h program. For larger volumes, the solvent was initially frozen in a glass vial using liquid nitrogen, and then freeze dried (Heto Lyolab 3000) for 2 h.

Mass Spectrometric Analysis

MALDI-TOF. An Applied Biosystems Voyager DE-Pro Biospectrometry Workstation Matrix-Assisted Laser Desorption/Ionisation Time of Flight (MALDI-TOF) mass spectrometer (Framingham, MA, USA) was used to obtain MALDI-TOF spectra of components within lyophilised fractions. Samples from fractions containing single components were prepared by diluting with matrix (37 mg THAP in 1 mL ACN, 45 mg ammonium citrate in 1 mL water – mixed 1 : 1) either 2 : 1, 1 : 1 or 1 : 5 (sample : matrix) prior to analysis. 1 μL of sample was spotted onto the MALDI target plate and allowed to dry. Samples were then analyzed in positive linear mode using delayed extraction (500 ns) and an

This journal is © The Royal Society of Chemistry 2011

Org. Biomol. Chem., 2011, **9**, 1632–1641 | 1639

accelerating voltage of 25 000 V. Acquisition was between 4000–15000 Da with 100 shots/spectrum.

EI-MS. EI-MS spectra were acquired on a Micromass Q-TOF Global Tandem Mass Spectrometer (Waters, Manchester, UK) fitted with a NanoSpray ion source. Negative mode was used for data acquisition, and the instrument was calibrated with ions produced from a standard solution of taurocholic acid (10 pmole μL^{-1}) in acetonitrile. The HPLC fractions collected were lyophilised (SpeedVac, Thermo Electron, UK) and mixed with a 1 : 1 v/v mixture of 40% acetonitrile–water and 20 mM triethylamine–water (TEA, Fischer Scientific, UK) which was also used as the electrospray solvent. 3–5 μL of sample was loaded into a metal-coated borosilicate electrospray needle with an internal diameter of 0.7 mm and a spray orifice of 1–10 μm (NanoES spray capillaries, Proxeon Biosystems, UK), and this was positioned ~10 mm from the sample cone to provide a flow rate of ~20 nL min^{-1}. Nitrogen was used as the API gas, and the capillary, cone and RF Lens 1 voltages were set to 1.8–2.0 kV, ~ 35 V and 50 V, respectively, to ensure minimum fragmentation of the ligand/DNA adducts. The collision voltage was set to 5 V and the MCP voltage to 2200 V. Spectra were acquired over the 100–1500 m/z range.

Circular Dichroism and Thermal Denaturation Studies. The UV & CD spectra of the oligonucleotides and oligonucleotide/ligand complexes were acquired on a Chirascan spectrometer (Applied Photophysics Ltd, Leatherhead, UK). The UV absorbance and CD spectra were measured between 500–200 nm in a strain-free rectangular 10 mm cell. The instrument was flushed continuously with pure evaporated nitrogen throughout the experiments. Spectra were recorded using a 0.5 nm step size, a 1.5 s time-per-point and a spectral bandwidth of 1 nm. Addition of ligand to the oligonucleotide solutions was carried out while maintaining a constant concentration of DNA. All spectra were acquired at room temperature and the buffer baseline corrected. All CD spectra were smoothed using the Savisky-Golay method, and a window factor of 4–12 was used for a better presentation.

For thermal denaturation experiments, the CD spectra were first recorded at room temperature (20 °C), then at the highest temperature (90 °C), and then again after cooling to 20 °C. Melting profiles were recorded during both the heating and cooling phases. The instrument was equipped with a Quantum (NorthWest, USA) TC125 Peltier unit set to change temperature from 20→90 °C at a rate of 3 °C min^{-1}, with a 5 °C step-size and a 0.2 °C tolerance. The same parameters were set for the cooling (90→20 °C) phases. A 2 s CD measurement time scale was employed. Temperature was measured directly with a thermocouple probe in the solutions. Melting temperatures were fitted using the Levenbert-Marquart algorithm for Van Hoff's isochors.

Molecular Modelling

Initial ligand structures were built using Maestro, and minimized with MacroModel (Schrodinger, LLC) using the MM3 charges and force field. Structures exported in PDB format were converted to the mol2 format suitable for use in Amber,[23] applying the Gasteiger charge method. Missing parameters were added with the 'parmchk' program. The DNA was constructed by means of the 'Nucgen' program, and hairpins were modelled with Amber.

GWL-78 (**1**) and anthramycin (**2**) were graphically aligned in the minor groove of the DNA using the 'Xleap' program so that the A-ring of the PBD was oriented towards the 3′-end of the helix, and the N10-nitrogen of the 7-membered ring was in close proximity to the NH_2 of guanine. Use was made of 'parm99' and the general Amber force field parameters 'gaff'. Subsequent minimization steps were performed with the DNA and unbound ligand using 'Sander' in such a way that the DNA was initially restrained with a high force constant, thus allowing the ligand to adjust to the DNA environment. Further minimization steps were then performed while gradually reducing the restraints to zero. The generalized Born/surface area (GB/SA) implicit solvent model was used with monovalent electrostatic ion screening simulated with SALTCON set to 0.2 M. A long range non-bonded cut-off of 100 (Å) was used. Final models were visualized with the VMD and PyMol[24] programs.

References

1 L. Cipolla, A. C. Araujo, C. Airoldi and D. Bini, *Anti-Cancer Agents in Medicinal Chemistry*, 2009, **9**, 1–31.
2 D. E. Thurston and D. S. Bose, *Chem. Rev.*, 1994, **94**, 433–465.
3 D. E. Thurston, in *Molecular Aspects of Anticancer Drug-DNA Interactions*, ed. S. Neidle and M. J. Waring, The Macmillan Press Ltd., London, UK, London, 1993, vol. 1, pp. 54–88.
4 A. Kamal, M. V. Rao, N. Laxman, G. Ramesh and G. S. K. Reddy, *Curr. Med. Chem.: Anti-Cancer Agents*, 2002, **2**, 215–254.
5 Dyeison Antonow and D. E. Thurston, *Chemical Reviews*, 2010, DOI: 10.1021/cr100120f.
6 S. J. Gregson, P. W. Howard, J. A. Hartley, N. A. Brooks, L. J. Adams, T. C. Jenkins, L. R. Kelland and D. E. Thurston, *J. Med. Chem.*, 2001, **44**, 737–748.
7 D. E. Thurston, "Chemisty and Pharmacology of Anticancer Drugs", CRC Press (Taylor & Francis), Boca Raton, Florida, USA, pp 281, (2007), [ISBN 0-8493-9219-5].
8 R. P. Hertzberg, S. M. Hecht, V. L. Reynolds, I. J. Molineux and L. H. Hurley, *Biochemistry*, 1986, **25**, 1249–1258.
9 K. M. Rahman, H. Vassoler, C. H. James and D. E. Thurston, *ACS Medicinal Chemistry Letters*, 2010, **1**, 427–432.
10 M. S. Puvvada, J. A. Hartley, T. C. Jenkins and D. E. Thurston, *Nucleic Acids Res.*, 1993, **21**, 3671–3675.
11 G. Wells, C. R. H. Martin, P. W. Howard, Z. A. Sands, C. A. Laughton, A. Tiberghien, C. K. Woo, L. A. Masterson, M. J. Stephenson, J. A. Hartley, T. C. Jenkins, S. D. Shnyder, P. M. Loadman, M. J. Waring and D. E. Thurston, *J. Med. Chem.*, 2006, **49**, 5442–5461.
12 M. S. Puvvada, S. A. Forrow, J. A. Hartley, P. Stephenson, I. Gibson, T. C. Jenkins and D. E. Thurston, *Biochemistry*, 1997, **36**, 2478–2484.
13 M. Kotecha, J. Kluza, G. Wells, C. C. O'Hare, C. Forni, R. Mantovani, P. W. Howard, P. Morris, D. E. Thurston, J. A. Hartley and D. Hochhauser, *Mol. Cancer Ther.*, 2008, **7**, 1319–1328.
14 W. Leimgrub, V Stefanov, F. Schenker, A. Karr and J. Berger, *J. Am. Chem. Soc.*, 1965, **87**, 5791–5793.
15 M. L. Kopka, D. S. Goodsell, I. Baikalov, K. Grzeskowiak, D. Cascio and R. E. Dickerson, *Biochemistry*, 1994, **33**, 13593–13610.
16 D. Antonow, M. Kaliszczak, G.-D. Kang, M. Coffils, A. C. Tiberghien, N. Cooper, T. Barata, S. Heidelberger, C. H. James, M. Zloh, T. C. Jenkins, A. P. Reszka, S. Neidle, S. M. Guichard, D. I. Jodrell, J. A. Hartley, P. W. Howard and D. E. Thurston, *J. Med. Chem.*, 2010, **53**, 2927–2941.

1640 | *Org. Biomol. Chem.*, 2011, **9**, 1632–1641

This journal is © The Royal Society of Chemistry 2011

17 L. H. Hurley, C. S. Allen, J. M. Feola and W. C. Lubawy, *Cancer Research*, 1979, **39**, 3134–3140.

18 K. M. Rahman, V. Mussa, M. Narayanaswamy, C. H. James, P. W. Howard and D. E. Thurston, *Chem. Commun.*, 2009, 227–229.

19 M. Narayanaswamy, W. J. Griffiths, P. W. Howard and D. E. Thurston, *Anal. Biochem.*, 2008, **374**, 173–181.

20 K. M. Rahman, A. S. Thompson, C. H. James, M. Narayanaswamy and D. E. Thurston, *J. Am. Chem. Soc.*, 2009, **131**, 13756–13766.

21 R. K. Malhotra, J. M. Ostrander, L. H. Hurley, A. G. McInnes, D. G. Smith, J. A. Walter and J. L. C. Wright, *J. Nat. Prod.*, 1981, **44**, 38–44.

22 K. M. Rahman and D. E. Thurston, *Chem. Commun.*, 2009, 2875–2877.

23 T. A. D. A. D. Case, T. E. III Cheatham, C. L. Simmerling, J. Wang, R. E. Duke, R. Luo, K. M. Merz, D. A. Pearlman, M. Crowley, R. C. Walker, W. Zhang, B. Wang, S. Hayik, A. Roitberg, G. Seabra, K. F. Wong, F. Paesani, X. Wu, S. Brozell, V. Tsui, H. Gohlke, L. Yang, C. Tan, J. Mongan, V. Hornak, G. Cui, P. Beroza, D. H. Mathews, C. Schafmeister, W. S. Ross; and P. A. Kollman, *Amber Version 9 Software*, University of California, San Francisco, 2006.

24 W. L. DeLano, The PyMol Molecular Graphics System, DeLano Scientific LLC, Palo Alto, CA, USA, 2008.

This journal is © The Royal Society of Chemistry 2011

Org. Biomol. Chem., 2011, **9**, 1632–1641 | 1641